J|A|C|S
ARTICLES
Published on Web 10/26/2002

Photoinduced Electron Transfer between a Carotenoid and TiO_2 Nanoparticle

Jie Pan,[†,‡] Gábor Benkö,[†] Yunhua Xu,[§] Torbjörn Pascher,[†] Licheng Sun,[§] Villy Sundström,[†] and Tomáš Polívka*[,†]

Contribution from the Department of Chemical Physics, Lund University, Box 124, S-22100 Lund, Sweden, Institute of Physics, Chinese Academy of Sciences, Beijing 100080, China, and Department of Organic Chemistry, Stockholm University, S-10691 Stockholm, Sweden

Received July 30, 2002

Abstract: The dynamics of photoinduced electron injection and recombination between all-*trans*-8′-apo-β-caroten-8′-oic acid (ACOA) and a TiO_2 colloidal nanoparticle have been studied by means of transient absorption spectroscopy. We observed an ultrafast (~360 fs) electron injection from the initially excited S_2 state of ACOA into the TiO_2 conduction band with a quantum yield of ~40%. As a result, the $ACOA^{\bullet+}$ radical cation was formed, as demonstrated by its intense absorption band centered at 840 nm. Because of the competing S_2-S_1 internal conversion, ~60% of the S_2-state population relaxes to the S_1 state. Although the S_1 state is thermodynamically favorable to donate electrons to the TiO_2, no evidence was found for electron injection from the ACOA S_1 state, most likely as a result of a complicated electronic nature of the S_1 state, which decays with a ~18 ps time constant to the ground state. The charge recombination between the injected electrons and the $ACOA^{\bullet+}$ was found to be a highly nonexponential process extending from picoseconds to microseconds. Besides the usual pathway of charge recombination forming the ACOA ground state, about half of the $ACOA^{\bullet+}$ recombines via the ACOA triplet state, which was monitored by its absorption band at 530 nm. This second channel of recombination proceeds on the nanosecond time scale, and the formed triplet state decays to the ground state with a lifetime of ~7.3 μs. By examination of the process of photoinduced electron transfer in a carotenoid-semiconductor system, the results provide an insight into the photophysical properties of carotenoids, as well as evidence that the interfacial electron injection occurs from the initially populated excited state prior to electronic and nuclear relaxation of the carotenoid molecule.

Introduction

Carotenoids are a class of natural pigments playing important roles in many biological systems extending from photosynthetic organisms to humans. In the photosynthetic antenna pigment−protein complexes, carotenoids act as accessory light-harvesting pigments and they efficiently transfer energy to (bacterio)-chlorophylls.[1,2] In the photosynthetic reaction center, they can play the role of electron donor when a suitable electron acceptor is available.[3,4] Besides light harvesting and electron transfer, another important function of carotenoids is photoprotection. They can effectively quench chlorophyll triplet states, and the formed triplet states of carotenoids are able to harmlessly dissipate the excess energy to the environment, preventing oxidative damage caused by formation of singlet oxygen because of interaction of $^3O_2$ with triplet states of chlorophyll.[5] An alternative protection mechanism operating also in other organisms including humans is a direct scavenging of singlet oxygen and other active radicals.[6]

Carotenoids contain a long conjugated carbon−carbon double bond chain with diverse end groups and substituents. Since their carbon backbone possesses C_{2h} symmetry, their strong absorption in the spectral region of 420−550 nm results from a transition between the ground-state S_0 ($1A_g^-$ in the idealized C_{2h} group) and the upper excited S_2 ($1B_u^+$) state. A transition between the S_0 and S_1 ($2A_g^-$) states is optically forbidden because of the symmetry selection rules.[7] Whereas the S_2 state undergoes fast internal conversion (IC) to the S_1 state within a few hundred femtoseconds,[8] the S_1 state has a lifetime ranging from 1 to 200 ps, depending on the number of conjugated carbon−carbon double bonds present in the molecule.[9] Because

* Corresponding author. E-mail: tomas.polivka@chemphys.lu.se. Fax: +46-46-222 4119. Telephone: +46-46-222 4700).
† Lund University.
‡ Chinese Academy of Sciences.
§ Stockholm University.

(1) Ritz, T.; Damjanović, A.; Schulten, K.; Zhang, J.-P.; Koyama, Y. *Photosynth. Res.* **2000**, *66*, 125 and references therein.
(2) van Amerongen, H.; van Grondelle, R. *J. Phys. Chem B* **2001**, *105*, 604 and references therein.
(3) Tracewell, C. A.; Cua, A.; Stewarr, D. H.; Bocian, D. F.; Brudvig, G. W. *Biochemistry* **2001**, *40*, 193.
(4) Faller, P.; Pascal, A.; Rutherford, A. W. *Biochemistry* **2001**, *40*, 6431.
(5) Farhoosh, R.; Chynwat, V.; Gebhard, R.; Lugtenburg, J.; Frank, H. A. *Photochem. Photobiol.* **1997**, *66*, 97.
(6) Edge, R.; McGarvey, D. J.; Truscott, T. G. *J. Photochem. Photobiol., B* **1997**, *41*, 189.
(7) Christensen, R. L. In *Photochemistry of Carotenoids*; Frank, H. A., Young, A. J., Britton, G., Cogdell, R. J., Eds.; Kluwer Academic Publishers: Dodrecht, The Netherlands, 1999; pp 137−159.
(8) Macpherson, A.; Gillbro, T. *J. Phys. Chem. A* **1998**, *120*, 5049.

of the short lifetime of singlet excited states and extremely low yield of the intersystem crossing (ISC) to the longer-lived triplet states,[10] carotenoids in solution are generally not photochemically reactive. However, as shown in numerous studies of natural photosynthetic light-harvesting systems, a carotenoid locked in an appropriate orientation relative to acceptor molecules such as chlorophyll in a protein matrix and having suitable energetics of the donor and acceptor can efficiently transfer excitation energy to the chlorophyll.[1,2] Recently, photoelectrochemical studies of assemblies consisting of carotenoid molecules in direct contact with conducting[11] or semiconducting[12] electrodes indicate that carotenoids can indeed act as photoactive species in photoinduced electron transfer (ET) processes when carefully incorporated into organized structures with some appropriate electron acceptors. While extensive studies of energy transfer processes involving carotenoids in proteins have been carried out,[1,2] the photoinduced ET from an excited carotenoid molecule is much less investigated. In this paper, our interest is to examine this process.

To study the photoinduced ET from carotenoid molecules, a suitable electron acceptor is required. As mentioned earlier, diffusion controlled bimolecular electron-transfer reactions between carotenoids and an electron acceptor in solution are not applicable because of the short lifetime of the carotenoid excited states. To overcome this kinetic limitation, we selected a semiconductor as electron acceptor, because (1) some semiconductors are efficient electron acceptors, as shown by numerous studies of dye-sensitized semiconductors;[13−15] (2) modified carotenoids can be directly attached to the semiconductor to achieve the desired ET reaction without involving diffusion processes; and, (3) perhaps the most important reason, the electron injection from the excited state of the dye into the conduction band of the semiconductor may compete with the relaxation of carotenoid excited states, since rates of electron injection on the order of $10^{11}-10^{13}$ s^{-1} were observed[13,14] in various dye-semiconductor systems including sensitizers such as translational metal compounds[16] and organic dyes.[17−21] A recent report demonstrated that the electron injection can occur from the initially excited nonthermalized singlet state of the dye, meaning that electron injection can successfully compete with intramolecular energy relaxation processes.[16]

The carotenoid-semiconductor interface is an unusual system. When compared to the previously studied sensitizers[13,14] that have excited states with known properties and long lifetimes (>1 ns), carotenoids typically have rather complex photophysics. Except the known lifetimes of the S_1 and S_2 states, there is little knowledge about IC processes occurring in the carotenoid molecule. Moreover, it was proposed that additional dark excited states might exist between the S_1 and S_2 excited states, resulting in even more complex pathways for energy deactivation processes.[22−24] Also, because of the forbiddeness of the S_0-S_1 transition, the energy of the carotenoid S_1 state was established only recently for a few carotenoids,[25,26] and the exact values of the S_1 energy are still a matter of debate.[27,28] Therefore, it is of interest to explore how the carotenoid S_2 and S_1 states are involved in the photoinduced ET process. Besides the mechanism and pathway of the photoinduced ET from carotenoids, the study of the carotenoid-semiconductor system may also provide new insights into the photophysical properties of carotenoids.

Scheme 1. Molecular Structure of 8′-apo-β-caroten-8′-oic-acid (ACOA)

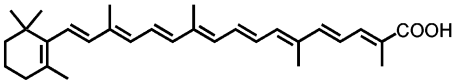

In the present work, we have studied the interfacial ET between 8′-apo-β-caroten-8′-oic-acid (ACOA, see Scheme 1) and TiO_2 colloidal nanoparticles by means of transient absorption spectroscopy. The TiO_2 is chosen as a semiconductor, since its conduction band is thermodynamically favorable to accept electrons from ACOA and there is a high density of states in its conduction band available to accept electrons.[13,14] The ACOA molecule with a terminal carboxylate group, modified from commercially available 8′-apo-β-carotenal, is used to accomplish an efficient attachment to the TiO_2 surface. Photophysical properties of the ACOA molecule bound to TiO_2 and the pathways of ET between ACOA and TiO_2 were characterized. The results will be explained by using the simplified energy level diagram shown in Figure 1. We have observed electron injection from the initially excited S_2 state to the TiO_2 (pathway 2), although part of the S_2 population undergoes IC to the S_1 state, followed by relaxation to the ground state (pathway 6 and 7). No evidence was found for electron injection from the S_1 state. Characterization of the ET processes was made by monitoring the dynamics of the oxidized ACOA ($ACOA^{\bullet+}$) and the recovery of the ground state. Interestingly, we have observed two channels for recombination between electrons in TiO_2 and the $ACOA^{\bullet+}$. Besides the recombination directly to the ACOA ground state (pathway 5), a part of the $ACOA^{\bullet+}$ molecules undergo recombination, forming the triplet state of ACOA (T_1), which then decays back to the ground state (pathways 8 and 9). Our findings provide information on the mechanism of photoinduced ET reactions for carotenoids and demonstrate another example of band-selective electron injection from a short-lived state.

(9) Frank, H. A.; Desamero, R. Z. B.; Chynwat, V.; Gebhard, R.; van der Hoef, I.; Jansen, F. J.; Lugtenburg, J.; Gosztola, D.; Wasielewski, M. R. *J. Phys. Chem. A* **1997**, *101*, 149.
(10) Nielsen, B. R.; Mortensen, A.; Jørgensen, K.; Skibsted, L. H. *J. Agric. Food Chem.* **1996**, *44*, 2106.
(11) Sereno, L.; Silber J. J.; Otero, L.; del Valle Bohorquez, M.; Moore, A. L.; Moore, T. A.; Gust, D. *J. Phys. Chem.* **1996**, *100*, 814.
(12) Gao, F. G.; Bard, A. J.; Kispert, L. D. *J. Photochem. Photobiol. A* **2000**, *130*, 49.
(13) Grätzel, M.; Moser, J.-E. Solar Energy Conversion. In *Electron Transfer in Chemistry*, Vol. V; Balzani V., Gould, I., Eds.; Wiley-VCH: Weinheim, Germany, 2001; pp 589−644 and references therein.
(14) Asbury, J. B.; Hao, E.; Wang, Y.; Ghosh, H. H.; Lian, T. *J. Phys. Chem. B* **2001**, *105*, 4545 and references therein.
(15) Kalyanasundaram, K.; Grätzel, M. *Coord. Chem. Rev.* **1998**, *77*, 347.
(16) Benkö, G.; Kallioinen, J.; Korppi-Tommola, J. E.; Yartsev, A. P.; Sundström, V. *J. Am. Chem. Soc.* **2002**, *124*, 489.
(17) Tachibana, Y.; Haque, S. A.; Mercer, I. P.; Durrant, J. R.; Klug, D. R. *J. Phys. Chem. B* **2000**, *104*, 1198.
(18) He, J.; Benko, G.; Korodi, F.; Polívka, T.; Lomoth, R.; Akermark, B.; Sun, L.; Hagfeldt, A.; Sundstrom, V. *J. Am. Chem. Soc.* **2002**, *124*, 4922.
(19) Moser, J.; Grätzel, M.; Sharma, D. K.; Serpone, N. *Helv. Chim. Acta* **1985**, *68*, 1686.
(20) Hilgendorff, M.; Sundström, V. *J. Phys. Chem. B* **1998**, *102*, 10505.
(21) Benkö, G.; Hilgendorff, M.; Yartsev, A. P.; Sundström, V. *J. Phys. Chem. B* **2001**, *105*, 967.
(22) Sashima, T.; Koyama, Y.; Yamada, T.; Hashimoto, H. *J. Phys. Chem. B* **2000**, *104*, 5001.
(23) Gradinaru, C. C.; Kennis, J. T. M.; Papagiannakis, E.; van Stokkum, I. H. M.; Cogdell, R. J.; Fleming, G. R.; Niederman, R. A.; van Grondelle, R. *Proc. Natl. Acad. Sci. U.S.A.* **2001**, *98*, 2364.
(24) Furuichi, K.; Sashima, T.; Koyama, Y. *Chem. Phys. Lett.* **2002**, *356*, 547.
(25) Polívka, T.; Herek, J. L.; Zigmantas, D.; Åkerlund, H.-E.; Sundström, V. *Proc. Natl. Acad. Sci. U.S.A.* **1999**, *96*, 4914.
(26) Fujii, R.; Onaka, K.; Kuki, M.; Koyama, Y.; Watanabe, Y. *Chem. Phys. Lett.* **1998**, *288*, 847.
(27) Polívka, T.; Zigmantas, D.; Frank, H. A.; Bautista, J. A.; Herek, J. L.; Koyama, Y.; Fujii, R.; Sundström, V. *J. Phys. Chem. B* **2001**, *105*, 1072.
(28) Josue, J. S.; Frank, H. A. *J. Phys. Chem. A* **2002**, *106*, 4815.

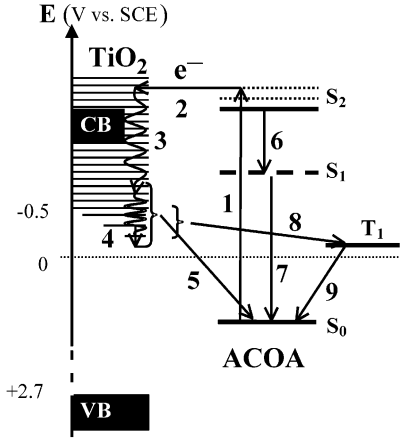

Figure 1. Schematic energy level diagram showing electron-transfer processes between the ACOA molecule and the TiO_2 particle. The diagram involves the ground state (S_0), two low-lying excited singlet states (S_1 and S_2), and the lowest excited triplet state (T_1) of the ACOA, conduction band (CB), and valence band (VB) of TiO_2. The redox potential of $ACOA^+$/ACOA was reported to be 0.68 V vs SCE in dichloromethane.[12] The energy level of the S_2 state in ACOA−TiO_2 was calculated by subtraction of the E_{0-0} of the S_0-S_2 transition (~ 2.64 eV) from the S_0 potential. The S_1 and S_2 energy difference was taken as ~7000 cm^{-1}, which was reported for the carotenoid violaxanthin having photophysical properties (S_1 lifetime, S_1-S_N spectrum) similar to those of ACOA.[25] The energy of the ACOA T_1 state (1^3B_u) was estimated as half of the S_1 energy according to the literature.[29] The energy of the CB is taken at pH = 2 in aqueous solution according to $E_{CB} = -0.1-0.059$ pH (vs NHE).[30] The different processes are indicated as follows: (1) photoexcitation; (2) electron injection; (3) electron relaxation and trapping within the CB (<100 fs);[31] (4) trapping/detrapping of the electron in states below the CB (>1 ns);[13] (5) electron recombination to S_0; (6 and 7) internal conversion from S_2 to S_1 and S_1 to S_0, respectively; (8 and 9) electron recombination to S_0 via T_1.

Experimental Section

Sample Preparation. All-*trans*-8′-apo-*β*-caroten-8′-oic acid (ACOA) was prepared according to the method described earlier[32] by oxidation of *trans*-8′-apo-*β*-caroten-8′-al (Fluka) with silver oxide, followed by chromatographic separation and recrystallization. The quality of the prepared compound was verified by NMR and mass spectroscopic measurements. An ACOA stock solution in dry ethanol was stored in the dark at −20 °C and was allowed to warm to room temperature just before use. Dry ethanol (analytical grade) was used without further purification.

The TiO_2 powder was prepared by controlled hydrolysis of $TiCl_4$ according to the procedure described earlier.[20,33] The quality of the obtained TiO_2 particles was tested by measuring the absorption spectrum of the TiO_2 colloidal solution. A plot of ln α (absorption coefficient) as a function of photon energy was analyzed following a method suggested by Kormann et al.,[33] yielding the band gap energy (E_g) of ~3.35 eV, which is similar to the value reported for particles with an average diameter of 2.4 nm.[33] The distribution in particle size can be estimated using the work of Serpone et al.,[34] where an average particle diameter of 2.1 nm with a variance of 1.1 nm was reported for TiO_2 particles obtained by a comparable preparation method. To form a colloidal TiO_2 solution, a suspension of 0.8 g/L TiO_2 was prepared by dissolving the desired amount of TiO_2 powder into a mixture of ethanol and water (97% EtOH). Before experiments, the ACOA ethanol solution (ACOA−EtOH) was added to the TiO_2 colloidal solution, and the mixture was degassed by nitrogen prior to measurements.

Spectroscopic Measurements. Steady-state absorption measurements were performed on a Jasco-V-530 spectrophotometer in a 0.2 cm path length quartz cuvette. The femtosecond spectrometer used in this study is based on an amplified Titanium/Sapphire laser system (Spectra Physics), with tunable pulses obtained from an optical parametric amplifier. The amplified Titanium/Sapphire laser system was operated at a repetition rate of 5 kHz, producing ~120 fs pulses with an average output power of ~1 W and a central wavelength of 800 nm. The amplified pulses were divided into two paths; one to pump an optical parametric amplifier (TOPAS, Light Conversion) for the generation of excitation pulses centered at 480 nm and the other to produce white-light continuum probe pulses in a 0.5 cm sapphire plate. For measurements at wavelengths above 1000 nm, instead of a white-light continuum, a second parametric amplifier was used to generate probe pulses, allowing measurements up to 1800 nm. To prevent sample degradation, the excitation pulses were attenuated to an energy of ~25 nJ/pulse by means of neutral density filters. The pump and probe pulses were allowed to overlap at the sample placed in a 2-mm path length quartz rotating cell. The pump beam was focused to a spot size of ~500 μm in diameter, corresponding to a photon density of ~ 6×10^{13} photons cm^{-2} $pulse^{-1}$. The mutual polarization of pump and probe beams was set to magic angle (54.7°). Absorption spectra were measured before and after measurements to ensure that no permanent photochemical changes occurred over the duration of the experiment.

For measurements on the slower time scale (nanosecond−microsecond), a laser flash photolysis experimental setup was used.[35] The excitation light was generated by a Quanta-Ray MOPO (λ = 450 nm, 0.6 mJ/pulse, 7 ns fwhm) pumped by a Quanta-Ray 210 Nd/YAG laser. The probe light was provided by a 75 W Xe arc lamp operated in either CW or pulsed mode. The excitation and probe beams were collinear. After passing through the sample placed in a 1 cm quartz cuvette, the probe light was spectrally filtered using two monochromators before being detected by a photomultiplier tube (PMT). For measurements in the visible and near-infrared spectral regions, a R928 and a R5108 PMT was used, respectively. A multiexponential analysis was used to quantify all the recorded kinetics. Individual kinetics were analyzed using deconvolution software Spectra Solve 2.01, Lastek Pty. Ltd. (1997), while a Matlab package (Nelder-Mead) was used for the global fitting of the traces.

Results and Discussion

Steady-State Absorption. Steady-state absorption measurements were performed to characterize the ACOA and its adsorption to the TiO_2 surface. Figure 2 shows the absorption spectrum of ACOA−EtOH and the effect of increasing the TiO_2 concentration. For ACOA−EtOH, a strong absorption appears between 350 and 500 nm with a maximum at 437 nm due to the S_0-S_2 transition. The vibrational structure is distinguishable with a peak-to-peak separation of ~1200 cm^{-1}, which is due to a mixture of C−C and C=C stretching modes of the carotenoid conjugated backbone.[36] The lowest 0−0 vibrational band of the S_0-S_2 transition is located at 460 nm. Upon addition of colloidal TiO_2 to the ACOA−EtOH, the absorption spectrum exhibits broadening and red shift, accompanied by a loss of vibrational structure. With increasing TiO_2 concentration, the absorption maximum shifts toward 446 nm and an isobestic point appears at 469 nm. The change of absorbance with TiO_2 concentration at a fixed wavelength was analyzed by employing the Langmuir adsorption isotherm according to ref 20, yielding an apparent association constant of $K_a = (5.9 \pm 1.1) \times 10^3$

(29) Truscott, T. G. *J. Photochem. Photobiol., B* **1990**, *6*, 359.
(30) Duonghong, D.; Ramsdan, J.; Grätzel, M. *J. Am. Chem. Soc.* **1982**, *104*, 2977.
(31) Huber, R.; Sporlein, S.; Moser, J. E.; Grätzel, M.; Wachtveitl, J. *J. Phys. Chem. B* **2000**, *104*, 8995.
(32) Singh, H.; John, J.; Cama, H. R. *Int. J. Vitam. Nutr. Res.* **1973**, *43*, 147.
(33) Kormann, C.; Bahnemann, D. W.; Hoffmann, M. R. *J. Phys. Chem.* **1988**, *92*, 5196.
(34) Serpone, N.; Lawless, D.; Khairutdinov, T. *J. Phys. Chem.* **1995**, *99*, 16646.
(35) Pascher, T. *Biochemistry* **2001**, *40*, 5812.
(36) Christensen, R. L.; Goyette, M.; Gallagher, L.; Duncan, J.; DeCoster, B.; Lugtenburg, J.; Jansen, F. J.; van der Hoef, I. *J. Phys. Chem. A* **1999**, *103*, 2399.

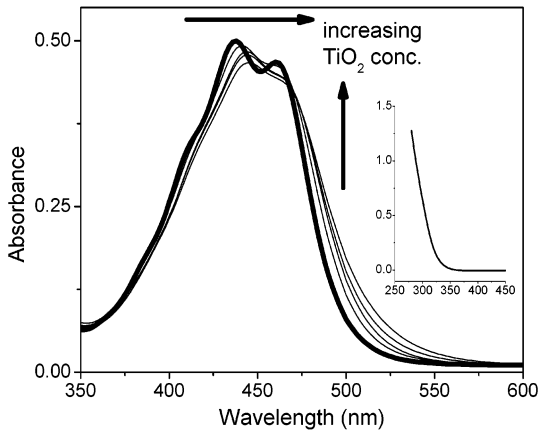

Figure 2. Absorption spectra of 30 μM ACOA in the presence of various TiO_2 concentrations in ethanol solution. The arrows indicate the effects of increasing TiO_2 concentration: 0 mM (bold line), 0.1 mM, 0.5 mM, 1.0 mM, and 3.0 mM, sequentially. Spectra were recorded with corresponding concentrations of TiO_2 colloidal solution as a blank in the reference path of the spectrometer. The absorption spectrum of the TiO_2 colloidal solution for the highest concentration (3 mM) is shown in the inset.

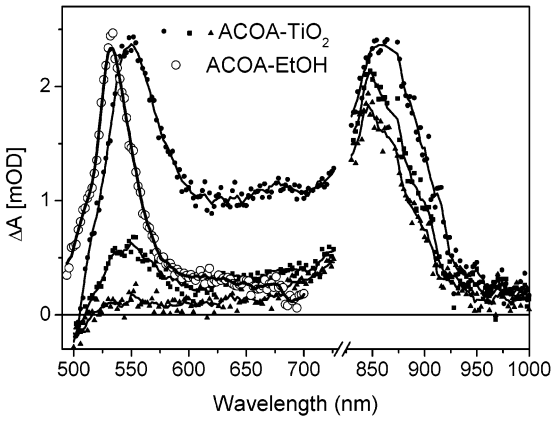

Figure 3. Visible and near-infrared transient absorption spectra of 30 μM ACOA with presence of 10 mM TiO_2 colloidal particles (ACOA−TiO_2) recorded at time delays of 6 ps (●), 40 ps (■), and 150 ps (▲) after excitation at 480 nm. The transient absorption spectrum of 30 μM ACOA in ethanol solution (ACOA−EtOH) measured at 6 ps (○) is shown for comparison. The transient absorption spectrum of the ACOA−EtOH is normalized to the maximum of the 6 ps transient absorption spectrum of the ACOA−TiO_2 system. Solid lines represent the results of a Fourier transform smoothing of the experimental data.

M^{-1} between ACOA and TiO_2 nanoparticles (data not shown), which is of the same order of magnitude as that found with other sensitizers with carboxylate group(s) adsorbed on TiO_2 particles.[37,38] Carboxylate group is usually employed as an anchor to the semiconductor surface, and the linkage modes of the formed surface complexes have been a subject of extensive investigations.[15,39] The distinct spectral changes and high association constant observed here imply a strong interaction between the ACOA molecules and the TiO_2 nanoparticles. Considering the hydrophobic character of the polyene chain and the hydrophilic property of the $COOH/COO^-$ end group, we believe the most likely interaction model between the ACOA and TiO_2 particle is that the $COOH/COO^-$ group of the ACOA molecule coordinates either directly or through a hydrogen bond to the TiO_2 surface,[15,39] while the conjugated backbone of ACOA sticks out from the TiO_2 surface into the solvent. This type of binding is also consistent with the recent characterization of thiol-substituted carotenoid self-assemblies on gold surfaces,[40] where similar spectral changes were observed.

Electron Injection. To characterize the interfacial ET process between the ACOA and TiO_2 (ACOA−TiO_2), we have used the free ACOA in ethanol solution (ACOA−EtOH) as a reference system, where no electron injection occurs. The transient absorption spectra recorded on the picosecond time scale, spanning the visible and near-infrared spectral range, are shown in Figure 3 for both ACOA−EtOH and ACOA−TiO_2. Given the subpicosecond S_2-S_1 relaxation, the transient absorption spectrum of ACOA−EtOH measured at 6 ps after excitation exhibits a strong absorption band because of excited-state absorption (ESA) from the carotenoid S_1 state. Its maximum at 535 nm corresponds well to the known S_1-S_N ESA band of carotenoids with a conjugation length similar to that of ACOA.[41] A similar band is observed also in the transient absorption spectrum recorded at 6 ps for ACOA−TiO_2, but the S_1 ESA band is slightly broader and its maximum is shifted to 550 nm. Besides the S_1 ESA at 550 nm, a spectrally broad and featureless ESA signal located between 600 and 700 nm appears in the case of ACOA−TiO_2. Such additional ESA bands were also reported for other dyes bound to the semiconductor surface, and their presence may be explained by a modification of higher excited states of the dye due to the interaction with the TiO_2 semiconductor.[21] The same situation obviously occurs in the ACOA−TiO_2 system studied here, since this additional ESA between 600 and 700 nm exhibits the same decay properties as the S_1 ESA at 550 nm (see Figure 3).

The most striking difference between the transient absorption spectra of ACOA−EtOH and ACOA−TiO_2 is observed in the near-infrared region above 750 nm. While the transient absorption spectra of carotenoids in solution do not show any distinct bands at 6 ps in this spectral region,[42] a strong band with a maximum at ~854 nm appears for the ACOA−TiO_2 system. The transient absorption spectra recorded at longer delay times still contain this band with a substantial intensity, which shows that it does not originate from the ACOA S_1 state (note that the blue shift of the absorption maximum with time toward 840 nm is due to the decay of the overlapping interaction-induced ESA in the region 600−700 nm). This is further confirmed by the kinetics recorded at 850 and 550 nm, which correspond to the new absorption band and the S_1 ESA, respectively, that exhibit different formation and decay kinetics (see below). It is known that the near-infrared region between 800 and 1000 nm is typical for the absorption of carotenoid radical cations.[43] Therefore, both the spectral position and the long lifetime of the 850 nm band suggests the generation of $ACOA^{\bullet+}$ through electron injection into the TiO_2.

To obtain detailed information about the temporal evolution of the bands observed in the transient absorption spectra in

(37) Kamat, P. V. *Chem. Rev.* **1993**, *93*, 267.
(38) Martini, I.; Hodak, J. H.; Hartland, G. V. *J. Phys. Chem. B* **1998**, *102*, 9508.
(39) Qu. P.; Meyer, G. J. Dye Sensitization of Electrodes. In *Electron Transfer in Chemistry*, Vol. IV; Balzani, V., Ed.; Wiley-VCH: Weinheim, Germany, 2001; pp 353−406.
(40) Liu, D.; Szulczewski, G. J.; Kispert, L. D.; Primak, A.; Moore, T. A.; Moore, A. L.; Gust, D. *J. Phys. Chem. B* **2002**, *106*, 2933.
(41) Frank, H. A.; Cua, A.; Chynwat, V.; Young, A.; Gosztola, D.; Wasielewski, M. R. *Photosynth. Res.* **1994**, *41*, 389.
(42) Zhang, J.-P.; Skibsted, L. H.; Fujii, R.; Koyama, Y. *Photochem. Photobiol.* **2001**, *73*, 219.
(43) Jeevarajan, J. A.; Wei, C. C.; Jeevarajan, A. S.; Kispert, L. D. *J. Phys. Chem.* **1996**, *100*, 5637.

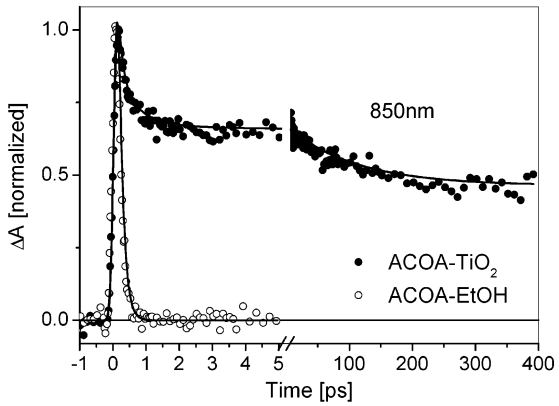

Figure 4. Transient absorption kinetics measured at 850 nm for the ACOA−TiO_2 (●) and ACOA−EtOH (○) systems after excitation at 480 nm. The symbols are experimental data points, and the solid curves are fits.

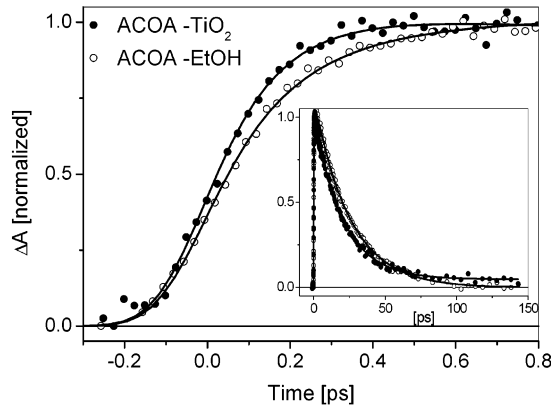

Figure 5. Rise kinetics of the S_1-S_N transition for both ACOA−TiO_2 at 550 nm (●) and ACOA−EtOH at 530 nm (○). The inset shows the corresponding full-scale traces. Solid lines represent the results of multiexponential fitting of the experimental data. Excitation was at 480 nm.

Figure 3, kinetics were measured at a few key wavelengths spanning both the visible and near-infrared region. The kinetic traces recorded in the near-infrared region at 850 nm for both ACOA−EtOH and ACOA−TiO_2 are shown in Figure 4. For ACOA−EtOH, the dynamics originates from the S_2-S_N transition[27,42] and reflects the instantaneous formation of the S_2 state followed by an ultrafast decay of the S_2 population. On the other hand, the 850 nm kinetics of the ACOA−TiO_2 system does not exhibit the characteristics of the carotenoid S_2 ESA. Except for the similar formation of the S_2 population and the initial subpicosecond decay of it, the signal at 850 nm has a very long lifetime, since at 400 ps only ∼30% of the amplitude at 1 ps has decayed, again suggesting the formation of a new species as a result of ET. The kinetic traces recorded at the maximum of the S_1 ESA showing the dynamics of the S_1 population (pathways 6 and 7 in Figure 1) are shown in Figure 5. Both the ACOA−EtOH and ACOA−TiO_2 exhibit a single-exponential decay with slightly different time constants of 25 ps (ACOA−EtOH) and 18 ps (ACOA−TiO_2), respectively. Also, the rise time of the S_1 ESA reflecting the S_2-S_1 relaxation exhibits differences between the ACOA−EtOH and ACOA−TiO_2 systems. While the rise time of the kinetics recorded at 535 nm for ACOA−EtOH can be fitted with a 180 fs time constant, a faster rise of ∼120 fs is observed in the case of the ACOA−TiO_2 (Figure 5). Because of the complex nature of the kinetic traces observed for the ACOA−TiO_2 system, a global fitting

Table 1. Global Fit Parameters for Kinetics Measured at Different Wavelengths in the ACOA−TiO_2 System[b]

fitted exponential components and amplitudes[a]					
wavelength (nm)	∼120 fs (%)	1.8 ps (%)	18 ps (%)	72 ps (%)	constant (%)
400	−1	9	58	17	16
550	−42		86	14	−1
850	33	5		17	45
950	76	11		6	7
1000	87	−1		7	6
1800	−3	25	63	11	1

[a] Negative amplitude means the rise component of the transient absorption signal, whereas components with positive amplitude mean the decay of the signal. [b] Excitation at 480 nm.

analysis of kinetics measured at several wavelengths (550, 850, 950, 1000, and 1800 nm, as well as the ground-state recovery at 400 nm) in the picosecond time window was performed. Four time components of 0.12, 1.8, 18, and 72 ps and one constant term were required to obtain satisfactory fits. The results are listed in Table 1 and discussed in detail in the following sections.

(1) Electron Injection from the ACOA S_2 State. A broad ESA band due to the S_2-S_N transition of carotenoids is known to appear in the near-infrared region.[27,42] However, because of the very short lifetime of the S_2 state in ACOA−EtOH (Figure 4), the S_2-S_N signal at 850 nm decays completely within 0.6 ps, and no ESA is observed at delays longer than 1 ps. Only the S_1 ESA bands in the visible part of the transient absorption spectrum are observable on the picosecond time scale for ACOA−EtOH. However, as shown in Figure 3, excitation of the ACOA−TiO_2 system gives rise to a long-lived absorption band located at ∼840 nm, which is absent from the corresponding signal of the free ACOA in EtOH. Consequently, the appearance of the 840 nm absorption band in the case of the ACOA−TiO_2 is related to the interaction between ACOA and the TiO_2 particle. As mentioned earlier, the near-infrared region is typical for carotenoid radical cation absorption,[43] and we have also observed the absorption band of the chemically oxidized ACOA in dichloromethane at ∼850 nm (see Supporting Information). Thus, we conclude that the absorption band at ∼840 nm in Figure 3 is attributed to the absorption of the $ACOA^{\bullet+}$, produced as a result of electron injection. Moreover, the constructed photovoltaic cell based on ACOA−TiO_2 directly confirms that the formation of $ACOA^{\bullet+}$ is due to ET.[12]

Apart from the $ACOA^{\bullet+}$ signal, the absorption of electrons injected into the TiO_2 conduction band was reported as a broad and weak band extending from ∼600 nm toward the near-infrared region.[44] Therefore, we have measured kinetics at 950, 1000, and 1800 nm in order to directly observe the signals corresponding to the injected electrons. The 950 and 1000 nm kinetics exhibit features similar to those observed at 850 nm, although the long-decay components have substantially lower amplitudes at 950 and 1000 nm (see Table 1), suggesting overlap with the much stronger S_2 ESA at earlier times, which prevents us from directly observing the rise of the electron signal. Similarly, the 1800 nm kinetics is dominated by a signal decaying with the ACOA S_1 lifetime (see Table 1), which is clearly due to the S_1-S_2 transition observed in this spectral region also for other carotenoids.[25,27] The absorption of electrons

(44) Rothenberger, G.; Fitzmaurice, D.; Grätzel, M. *J. Phys. Chem.* **1992**, *96*, 5983.

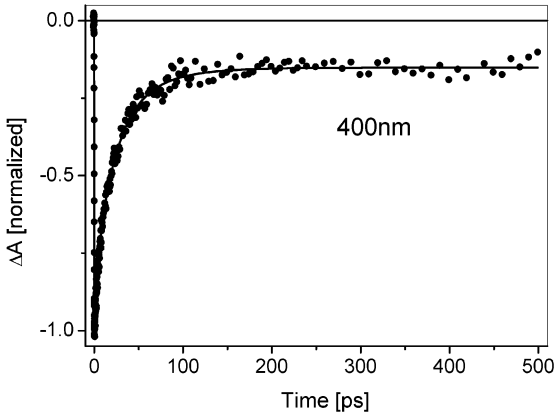

Figure 6. Transient absorption kinetics of ground states bleaching recovery (GSR) for ACOA−TiO_2 in ethanol solution measured at 400 nm after 480 nm excitation. The solid line represents the fitting result.

injected into the TiO_2 can be observed in the near-infrared region, as demonstrated by the presence of long time components in this spectral region, providing additional proof that the ET from the ACOA into TiO_2 indeed occurs.

In Table 1, the subpicosecond component of ~120 fs corresponds to the fast decay of the ACOA−TiO_2 S_2 absorption observed at 850, 950, and 1000 nm and to the rise of the S_1 ESA at 530 and 1800 nm. On the other hand, the fitting of the rise at 535 nm for the ACOA−EtOH yields a 180 fs component. Since the rise of the S_1 state is associated with the decay of the initially excited S_2 state, the faster S_1 rise of the ACOA−TiO_2 compared to that of the ACOA−EtOH indicates an additional quenching channel of the ACOA S_2 state in the presence of TiO_2. This is clear evidence that the initially photoexcited ACOA S_2 state undergoes both electron injection to TiO_2 and IC to the S_1 state (pathways 2 and 6 in Figure 1). Therefore, the transient absorption spectra recorded at picosecond time delays for ACOA−TiO_2 exhibit both the absorption in the near-infrared region due to the absorption of $ACOA^{\bullet+}$ and also the band with a maximum at 550 nm due to the S_1 ESA (Figure 3).

The rate constant related to the observed ~120-fs decay of the ACOA−TiO_2 S_2 state reflects the sum of the rates of electron injection from the S_2 state (k_{inj}) and the IC (k_{IC}) to the S_1 state: $^1/_{120}$ $fs^{-1} = k_{inj} + k_{IC}$. Using the S_1 state rise time of 180 fs observed for ACOA−EtOH for the value of k_{IC}, the equation yields $k_{inj} = {}^1/_{360}$ fs^{-1}, which gives an ~33% quantum yield of the electron injection. The obtained value is slightly lower than the ~50% yield estimated from a comparison of the absolute magnitudes of the S_1 ESA bands of ACOA−TiO_2 and ACOA−EtOH (assuming that the S_1 ESA extinction coefficient is not changed by the attachment). An ~40% yield of electron injection can be also estimated from the contribution of S_1 decay to the ground-state bleaching recovery (GSR) at 400 nm (see Figure 6 and Table 1). However, it should be pointed out that the ~120 fs rise component observed for the ACOA−TiO_2 system is on the edge of our time resolution (instrument response function ~200 fs). In addition, the amplitude of this rise is only 42%; thus, the actual time constant is most likely faster making the ~33% yield of the electron injection rather the lower limit of estimation. Nonetheless, it is clear that the ultrafast electron injection to the TiO_2 particle indeed occurs from the initially populated ACOA S_2 state. Unlike other sensitizers, for which the electron injection is fast compared with the overall relaxation processes allowing to achieve the electron injection quantum yield of nearly unity, in the case of ACOA, ~60% of the S_2 population decays to the S_1 state by IC (pathway 6 in Figure 1). In this respect, the ACOA−TiO_2 system is similar to the $Ru(dcbpy)_2(NCS)_2$ (i.e., RuN3)−TiO_2 nanoparticle film, in which an ultrafast electron injection (<50 fs) from the initially photoexcited singlet state effectively competes with the ~70-fs ISC to the triplet state.[16] Hence, besides the metal−polypyridyl complexes,[16,45,46] the ACOA−TiO_2 system is another example of efficient competition between electron injections with intramolecular relaxation processes as a result of photosensitization of a wide band gap semiconductor.

(2) S_1 State Dynamic of ACOA Bound to TiO_2 Surface. As we discussed earlier, a significant part of the initially excited S_2 state population of ACOA−TiO_2 does not inject electrons to TiO_2, but undergoes IC to the S_1 state (pathway 6 in Figure 1). Consequently, the possibility of electron injection from the ACOA S_1 state to the TiO_2 becomes important in terms of the effective conversion of the light absorbed by ACOA into the energy of spatially separated charges.

The S_1 state ESA of ACOA−TiO_2 shows similar spectral features as those recorded for ACOA−EtOH, except it is slightly broader and red-shifted (Figure 3) because of the interaction caused by the attachment to the surface of the TiO_2 particle. These spectral changes provide additional proof that the ACOA molecules excited under our experimental condition were indeed attached to the TiO_2 surface. The S_1 state lifetime of 25 ps for the ACOA in ethanol is in good agreement with that of other carotenoids with a similar conjugation length.[25,41] The shortening of the S_1 lifetime for the ACOA−TiO_2 to 18 ps (see Figure 5 and Table 1) might suggest that the S_1 state could be also a potential electron donor. However, no corresponding rise component of the $ACOA^{\bullet+}$ signal at 850 nm was observed (Figure 4 and Table 1), clearly showing that the shortening of the ACOA−TiO_2 S_1 lifetime is not due to electron injection but is rather a result of the interaction with the surface. In summary, even though both the ACOA S_2 and S_1 states are thermodynamically favorable for the donation of electrons to TiO_2 (see Figure 1), there is no electron injection occurring from the S_1 state.

The lack of the S_1 electron injection is consistent with a recent report that the generation of the β-carotene radical cation by ET to chloroform solvent occurs only from the initially populated S_2 state.[47] As mentioned in that work, the key to understanding the inability of the S_1 state to donate electrons might be the markedly different properties of the S_1 and S_2 states. While the S_2 state is a singlet excited state with ionic character, the S_1 state is a covalent state that can be described as involving two triplet excitations which are coupled to an overall singlet state.[48] The results shown here imply that the markedly different electronic properties of these two states affect their participation in the electron-transfer process.

It is worth noting that the nearly unit quantum yield of the electron injection process in RuN3−TiO_2 has been found partly because of the ability of RuN3 to inject electrons also from the thermalized triplet state.[16] It was found also for other dyes that the triplet state is not an effective electron donor to TiO_2,

(45) Ferrere, S.; Gregg, B. A. *J. Am. Chem. Soc.* **1998**, *120*, 843.
(46) Moser, J. E.; Grätzel, M. *Chimia* **1998**, *52*, 160.
(47) Zhang, J.-P.; Fujii, R.; Koyama, Y.; Rondonuwu, F. S.; Watanabe, Y.; Mortensen, A.; Skibsted, L. H. *Chem. Phys. Lett.* **2000**, *326*, 33.
(48) Tavan, P.; Schulten, K. *Phys. Rev. B* **1987**, *36*, 4337.

although it is thermodynamically possible.[18−21] The remarkable difference between the triplet states of the Ru−polypyridine complex and other organic dyes is that the former has a high degree of charge-transfer character and mixed singlet/triplet character.[13,15,17] This complicated and mixed electronic nature of the excited state may result in different couplings between the energy levels of the different excited donor molecules and acceptor semiconductor particle.[13−16,18−21] Accordingly, in the ACOA−TiO_2 system, it is likely that the double-triplet character of the ACOA S_1 state prevents efficient electron injection.

Electron Recombination. Earlier, we have demonstrated that the electron injection occurs from the initially excited ACOA S_2 state in concert with the IC to S_1 (pathways 2 and 6 in Figure 1). We now focus on the back ET from TiO_2 to $ACOA^{\bullet+}$. Besides recombination forming the ground-state ACOA (pathway 5 in Figure 1), $ACOA^{\bullet+}$ can undergo another channel of electron recombination, producing the triplet state of ACOA, which decays back to the ground state in a few microseconds (pathways 8 and 9 in Figure 1).

(1) Electron Recombination to the ACOA Ground State. The charge recombination between $ACOA^{\bullet+}$ and the conduction band electrons can be characterized by monitoring either the decay of the $ACOA^{\bullet+}$ absorption at 850 nm or the GSR at 400 nm. In Table 1, the global fitting analysis results in three exponential decay times of 0.12 ps (33%), 1.8 ps (5%), and 72 ps (17%) and a nondecaying component (45%) for the 850 nm kinetic trace. The subpicosecond component was assigned above to the ACOA−TiO_2 S_2 lifetime. Since no injection occurs on time scales longer than 1 ps, the signal at this wavelength after 1 ps is solely due to the decay of $ACOA^{\bullet+}$ caused by the electron recombination. The 1.8 and 72 ps components were found in both 850 and 400 nm kinetics with comparable amplitudes (see Table 1), indicating that a small fraction of $ACOA^{\bullet+}$ recombines to the ACOA ground state already on the picosecond time scale (pathway 5 in Figure 1). Despite the picosecond recombination, a majority of the formed $ACOA^{\bullet+}$ does not recombine within the first 400 ps, as shown by the presence of a nondecaying component in both 850 and 400 nm kinetics, demonstrating the nonexponential nature of the electron recombination process (Figures 4 and 6).[13,17,21]

Since the transient absorption measurements performed on the picosecond time scale are not capable of covering the full time evolution of the electron recombination process in the ACOA−TiO_2 system, measurements utilizing laser flash photolysis on a slower time scale (nanosecond−microsecond) were performed. The flash photolysis experiment on ACOA−EtOH does not produce any signal on these time scales because of the picosecond lifetime of ACOA in solution. The transient absorption spectra of the ACOA−TiO_2 were recorded in the 360−1000 nm spectral range (data shown in the Supporting Information), and a global fitting analysis on all 42 kinetic traces obtained in this spectral region was performed. To make visualization and interpretation of the results easier, in Figure 7a are shown the spectra obtained by calculations of the amplitudes (A_i) of a global four-exponential fit $\Delta\text{Abs} = \Sigma_{i=1}^{4} A_i e^{-k_i t}$ ($k_1 = {}^1/_{98}$ ns, $k_2 = {}^1/_{770}$ ns, $k_3 = {}^1/_{7.3}$ μs, $k_4 = {}^1/_{130}$ μs) on the measured transient absorption kinetics. The amplitude of each of the presented spectra is given by $S_j = \Sigma_{i=j}^{4} A_i$ and the difference between the two consecutive spectra shows the changes that occurred during the process with rate k_i.[49,50] For example, the first spectrum (S_1) is the sum of A_1 to A_4, thus depicting the transient absorption spectrum at time zero of the nanosecond laser pulse excitation. A strong absorption band appears in the infrared region with the same maximum of 840 nm, as that observed in the transient absorption spectrum recorded at 150 ps (Figure 3), which was identified as the absorption of $ACOA^{\bullet+}$. The multiexponential analysis shows that the 840 nm signal due to $ACOA^{\bullet+}$ is maintained from picoseconds to tens of microseconds, signaling that a long-lived charge separated state between the oxidized carotenoid molecule and the TiO_2 particle was achieved.

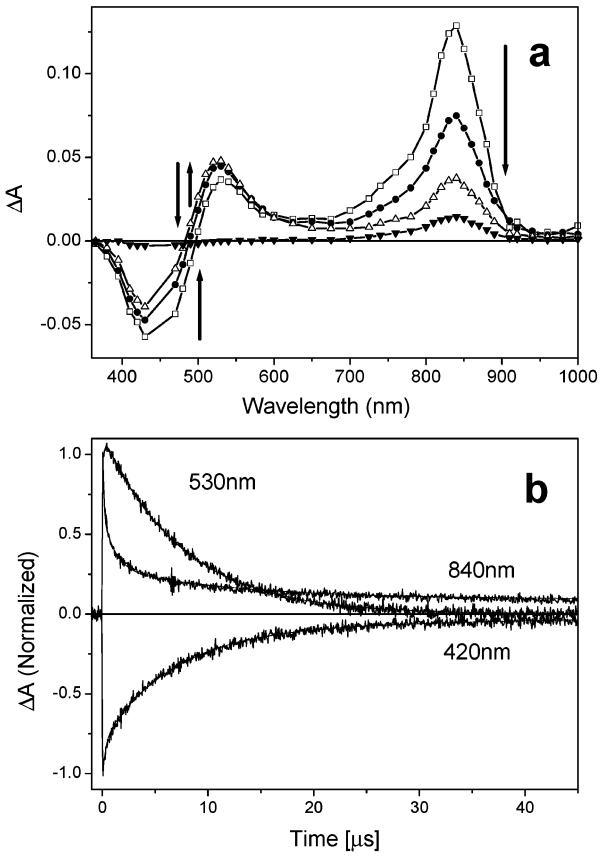

Figure 7. (a) Spectra obtained from a global four exponential fit ($\Delta\text{Abs} = \Sigma_{i=1}^{4} A_i e^{-k_i t}$, $k_1 > k_2$, $k_2 > k_3$, $k_3 > k_4$) of transient absorption kinetics measured for 5 μM ACOA in the presence of 10 mM TiO_2 colloidal particle in ethanol solution excited at 450 nm with 7-ns pulses (0.6 mJ/pulse). The presented spectra are shown in terms of amplitudes of individual time components by $S_j = \Sigma_{i=j}^{4} A_i$ as follows: S_1 (○), S_2 (●), S_3 (△), and S_4 (■). The arrows indicate the spectral changes with time. (b) Nanosecond−microsecond decay kinetics of ACOA−TiO_2 measured at 420 nm (GSR), 530 nm (T_1 decay), and 840 nm ($ACOA^{\bullet+}$ decay). The solid curves are fits. See text for details.

The highly nonexponential nature of the electron recombination, with kinetic components ranging from picoseconds to even milliseconds, has been reported in previous works,[13] and the behavior was attributed mainly to both spatial and energetic distribution of the trapped electrons in the nanoparticle.[13] As a result, the recombination is primarily controlled by the trapping/detrapping dynamics of electron transport within the particle. In the case of ACOA−TiO_2, a few of the injected electrons may become localized in traps with a strong electronic coupling

(49) Beechem, J. M. *Methods Enzymol.* **1992**, *210*, 37.
(50) Johnson, M. L.; Faunt, L. M. *Methods Enzymol.* **1992**, *210*, 1.

to the carotenoids and, therefore, recombine rapidly. If we compare these results with the recombination kinetics in RuN3-sensitized TiO_2 films, in which there is no recombination up to the microsecond time scale,[13,17] the charge recombination in the ACOA−TiO_2 system is considerably faster. This faster charge recombination together with an only ∼40% quantum yield of electron injection from the excited ACOA are the factors limiting the performance of the photovoltaic cell on the basis of ACOA-sensitized TiO_2 film.[12] However, it is worth noting that the blue-shift of the ACOA absorption spectrum when attached to the TiO_2 film in ref 12 suggests an aggregation of the ACOA molecules,[51] which questions a direct comparison with the results obtained here.

(2) Electron Recombination to the ACOA Triplet State. The charge recombination between the injected electrons in TiO_2 and $ACOA^{\bullet+}$ does not only generate the ACOA ground state, because, as shown in Figure 7b, the kinetics of $ACOA^{\bullet+}$ decay at 840 nm and the 420 nm kinetics representing GSR in ACOA−TiO_2 are not fully correlated. Moreover, a new absorption band appears at around 530 nm in the nanosecond−microsecond transient absorption spectra (Figure 7a). It is worth noting that this band clearly differs from the S_1 ESA band in the transient absorption spectra measured at a 6 ps delay (Figure 3) because the 530 nm band observed on the microsecond time scale is blue-shifted by about 20 nm from the 550 nm band recorded on the picosecond time scale. Also, the 550 nm band shown in Figure 3 disappears completely within 100 ps and, therefore, cannot be observed on the microsecond time scale. Contrary to the multiexponential decay observed at 840 nm, the decay of the 530 nm signal can be successfully fitted with a single component of 7.3 μs. In addition, the 7.3 μs lifetime of this band can be substantially shortened by the presence of oxygen in the sample (data not shown). All the observed features of the 530 nm band (spectral position, lifetime and sensitivity to oxygen) are in a good agreement with the known properties of carotenoid triplet states.[52] Thus, we conclude that the transient absorption band at ∼530 nm (see Figure 7) is due to the formation of the triplet state of ACOA (T_1).

From the amplitude sequence spectra in Figure 7a and kinetics at 530 nm in Figure 7b, it is evident that the T_1 state signal was only partially formed within the 7 ns laser pulse because the 530 nm band exhibits a rise even after the transient spectrum at time zero. To track the rise of this signal, kinetics at 530 nm were measured in the time window up to 700 ps (Figure 8). The initial 18 ps decay of the S_1-S_N ESA is followed by a slow rise occurring on the time scale extending from hundreds of picoseconds to nanoseconds, implying that the main part of T_1 is formed within this time window. Since the quantum yield of the intersystem crossing from the carotenoid singlet to triplet state in solution is very low (measurements on ACOA−EtOH failed to produce this absorption band),[10] the formation of T_1 is related to the interaction between ACOA and TiO_2. Thus, T_1 can be formed either from the S_1 state assuming an increase of the intersystem crossing quantum yield by the attachment or by recombination of the $ACOA^{\bullet+}$. Knowing the 18-ps lifetime of the S_1 state and the nanosecond formation of the T_1 state,

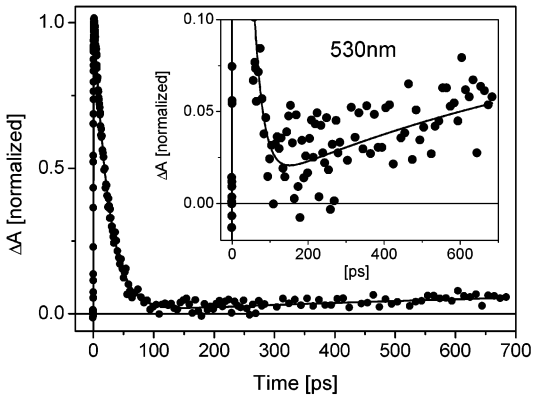

Figure 8. Transient absorption kinetics for ACOA−TiO_2 in ethanol solution measured at 530 nm. Inset: enlargement of the data at longer times. The symbols are experimental data points, and the solid curves are fits.

we can rule out the formation of the triplet by intersystem crossing. Besides, the presence of the 18 ps component in the 400 nm kinetics representing bleaching recovery clearly shows that the S_1 state indeed decays back to the ground state (Figure 6 and Table 1). Thus, we conclude that the ACOA triplet state is produced as a result of the back ET from $ACOA^{\bullet+}$, forming a second channel for electron recombination (pathway 8 in Figure 1).

The presence of this alternative pathway of electron recombination from $ACOA^{\bullet+}$ to triplet state ACOA is also supported by a closer inspection of the initial part of the nanosecond−picosecond kinetics at 420 nm (GSR), 840 nm (decay of $ACOA^{\bullet+}$), and 530 nm (ACOA T_1 state) shown in Figure 7b. The GSR kinetics is slower than the initial decay of the $ACOA^{\bullet+}$signal at 840 nm, and a distinguishable rise is observable for the 530 nm trace, signaling that the decay of $ACOA^{\bullet+}$ on the nanosecond time scale does not completely recombine to form the ground state but rather partially produces the triplet state (pathway 8 in Figure 1). The triplet state then decays monoexponentially to the ground state with a lifetime of 7.3 μs (pathway 9 in Figure 1). From the contribution of the 7.3 μs component to the GSR kinetics, we can estimate that more than 50% of $ACOA^{\bullet+}$ decays via the triplet channel of electron recombination.

Charge recombination via the triplet state of a carotenoid was already observed in other systems. In an artificial system consisting of a triad of carotenoid−porphyrin−fullerene mimicking the charge separation of the photosynthetic reaction center,[53,54] the back electron transfer to the ground state involved a higher driving force in the Marcus inverted region; thus, the charge recombination to yield the triplet was kinetically more favorable. The formation of the triplet state of a retinoid acid adsorbed to a TiO_2 nanoparticle suggested to be due to the charge recombination was reported, but no clear evidence for a precursor for this reaction was observed.[55]

Slow charge recombination between the oxidized dye and the electrons injected in the semiconductor was explained by both the Marcus inverted ET behavior and the dynamic of the

(51) Gruszecki, W. I. In *Photochemistry of Carotenoids*; Frank, H. A., Young, A. J., Britton, G., Cogdell, R. J., Eds.; Kluwer Academic Publishers: Dodrecht, The Netherlands, 1999; pp 363−379.
(52) Nielsen, B. R.; Jørgensen K.; Skibsted, L. H. *J. Photochem. Photobiol. A* **1998**, *112*, 127.
(53) Kuciauskas, D.; Liddell, P. A.; Lin, S.; Stone, S. G.; Moore, A. L.; Moore, T. A.; Gust, D. *J. Phys. Chem. B* **2000**, *104*, 4307.
(54) Carbonera, D.; Di Valentin, M.; Corvaja, C.; Agostini, G.; Giacometti, G.; Liddell, P. A.; Kuciauskas, D.; Moore, A. L.; Moore, T. A.; Gust, D. *J. Am. Chem. Soc.* **1998**, *120*, 4398.
(55) Weng, Y.-X.; Li, L.; Liu, Y.; Wang, L.; Yang, G.-Z.; Sheng, J.-Q. *Chem. Phys. Lett.* **2002**, *355*, 294.

trapping and detrapping of electrons in the semiconductor.[13] The driving force for the back electron transfer from the TiO_2 conduction band edge to form the ACOA ground state is estimated as $\Delta G \approx -1.2$ eV (see energy level scheme in Figure 1), which is in the Marcus inverted region for this reaction (the total reorganization energy λ associated with the heterogeneous charge transfer process is typically about 0.5 eV).[13] The triplet state of a carotenoid, however, is located approximately at half the energy of the S_1 state, leading to the triplet state of ACOA being located about 0.9 eV above the ground state. Therefore, the electron recombination to yield the ACOA triplet in the ACOA−TiO_2 system is consistent with the observations that the ET process forming excited products becomes the active pathway when its driving force is closer to reorganization energy than that of a reaction forming ground-state products.[56]

If we compare these results with other organic dye sensitizers, in which the ground state is usually the only electron acceptor for the back ET, the two-channel electron recombination involving a high yield of triplet state formation observed in this study is interesting. Since this feature is potentially interesting for regulating recombination processes in solar cells, various factors controlling the ratio between the two recombination channels such as excitation intensity, carotenoid structure, or crystallinity of TiO_2 needs to be addressed in future studies.

Conclusions

In summary, we have studied photophysical properties and photoinduced electron-transfer processes of ACOA molecules attached to an electron acceptor with a high density of acceptor states, that is, to TiO_2 nanoparticles. When bound to the surface, the ACOA molecules inject electrons from the initially excited S_2 state into the conduction band of the semiconductor on a few hundreds of femtoseconds time scale with a quantum yield of 40%, while a part undergoes competitive internal conversion to the S_1 state. Presumably because of the different electronic properties of the S_1 state, no electron injection occurs from this state, which further relaxes to the ground state. The product of the electron injection, $ACOA^{\bullet+}$, recombines with conduction band electrons to regenerate the ACOA ground state by two different channels. For about half of the $ACOA^{\bullet+}$ population, the charge recombination forms directly the ground state on a time scale extending from picoseconds to tens of microseconds, while the rest recombines to produce the ACOA triplet state on the nanosecond time scale, which subsequently relaxes to the ground state within a few microseconds.

Acknowledgment. The authors thank Dr. Chunxi Zhang for technical assistance and useful comments. J.P. thanks Prof. Guo-Zhen Yang from the Institute of Physics, Chinese Academy of Sciences for his support. This research was funded by grants from the Delegationen för Energiförsörjning i Sydsverige (DESS), the Swedish Research Council, the Knut and Alice Wallenberg Foundation, the Crafoord Foundation, and the Trygger Foundation.

Supporting Information Available: Absorption spectrum of chemically formed $ACOA^{\bullet+}$ radical cation and nanosecond−microsecond transient absorption spectra of the ACOA−TiO_2 system at all measured delays. This material is available free of charge via the Internet at http://pubs.acs.org.

JA0279186

(56) Winkler, J. R.; Di Bilio, A. J.; Farrow, N. A.; Richards, J. H.; Gray, H. B. *Pure Appl. Chem.* **1999**, *71*, 1753.